Uncertainty Estimation of Temperature Coefficient Measurements of PV Modules

Blagovest Mihaylov, Thomas R. Betts, Alberto Pozza, Harald Müllejans, and Ralph Gottschalg

Abstract—Temperature coefficients (TCs) of photovoltaic (PV) modules play an important role in distinguishing between products in an increasingly competitive market. However, measurement setups vary greatly, and interlaboratory comparisons show deviations from the mean of around ±10–15%, or even larger, for temperature coefficients of maximum power. Measurement deviations often do not agree with the uncertainty estimates, indicating that uncertainty is significantly underestimated. On the other hand, some laboratories have adopted a very conservative approach and needlessly overestimate the uncertainty. A new and robust methodology for calculating the temperature coefficients is presented here. This includes estimating and propagating the uncertainty of different types of measurement systems and procedures, in accordance with international standards. The method is validated with a round-robin intercomparison. Two c-Si modules were measured with five different measurement setups with uncertainties estimated following the proposed approach. The advanced uncertainty estimation method resulted in a decrease of the estimated uncertainty of all systems by a minimum of 50%, compared with the previous conservative estimates, enabling us to identify a previously unknown systematic effect. The measurement results of one of the systems were inconsistent with the estimated uncertainty. Further investigation confirmed a systematic effect due to the poor spectrum of that system. Removing the outlier measurement, the measurement percentage deviation from the reference value for maximum power temperature coefficients was within ±3.2%. The deviation was consistent with the stated uncertainties. The approach can facilitate the reduction of temperature coefficient measurement uncertainty by highlighting areas of improvement for bespoke systems.

Index Terms—Measurement, module, photovoltaic (PV), temperature coefficient (TC), uncertainty.

I. Introduction

TEMPERATURE COEFFICIENT (TC) measurements are required for accurate energy yield estimates and module energy ratings. However, the measurement deviation from the mean of maximum power TC, i.e., δ, between laboratories is reported to be ±10–15% or even larger in a number of intercomparisons [1]–[3]. Furthermore, the measurement uncertain-

ties are frequently neglected or the measurement deviation in round-robin intercomparisons is outside stated uncertainties. A ±15% difference in measurement of the maximum power TC of a typical c-Si module with a TC around –0.45%/°C corresponds to ±0.0675%/°C. This translates to a difference in predicted power at 55 °C of ±2%. In an increasingly competitive marketplace, this level of measurement deviation and large uncertainty is not acceptable.

The challenges in measuring TCs were reported in [4] and [5]; however, they are not always considered in the uncertainty estimations provided by laboratories. The methodology for estimating the uncertainty for I_{SC}, V_{OC}, and P_{MAX} measurements at standard test conditions (STC) has been standardized over the years [6]–[10]. This led to a reduction in the measurement deviation by enabling the identification of critical contributions to measurement uncertainty and improvements to experimental facilities reducing their contribution. Consequently, a better agreement between measurement laboratories within their stated uncertainties was achieved [11]. Therefore, the first step in improving TC measurements is to have a robust uncertainty estimation methodology and a consistent way of calculating the TC. Often inappropriate linear fits are used due to a lack of understanding of the underlying assumptions about the data. When these assumptions do not apply, the fit is invalid. The appropriate measurement standard IEC 60891 [12] does not specify the exact type of linear fit to be used. Most commonly, the temperature measurements are assumed to have negligible uncertainty, and an ordinary least-squares fit is used. This not only results in a significant underestimation of the uncertainty but in an incorrectly calculated TC as well.

The approach at the Centre for Renewable Energy Systems Technology (CREST) for estimating and propagating the uncertainties in TC measurements overcomes these issues. A discussion of the previous approach and the measurement system at CREST can be found in [13]. The approach has been further developed to apply separate effective temperature measurements and to include correlations between measurements at different temperatures. Consideration of correlations is necessary, since the common practice of using relative uncertainties was shown using Monte Carlo simulations (unpublished work) to result in an underestimation.

In this paper, the details of calculating the uncertainties of TC measurements in the most general case in accordance with international standards are presented. The approach was validated via a round-robin of two modules measured on five different measurement systems with uncertainty estimates calculated following the proposed approach. Both the deviation in the calculated TCs and the uncertainties were reduced compared with the previous methods used.

B. Mihaylov, T. R. Betts, and R. Gottschalg are with the Centre for Renewable Energy Systems Technology, Loughborough University, Loughborough LE11 3TU, U.K. (e-mail: B.V.Mihaylov@lboro.ac.uk; T.R.Betts@lboro.ac.uk; R.Gottschalg@lboro.ac.uk).

A. Pozza and H. Müllejans are with the Joint Research Centre, European Solar Test Installation I-21027, Ispra Italy (e-mail: Alberto.Pozza@jrc.ec.europa.eu; Harald.MUELLEJANS@ec.europa.eu).

II. TEMPERATURE COEFFICIENT MEASUREMENT SETUPS

TC measurements involve measuring the performance parameters of modules at different module temperatures and performing a regression to calculate the derivative with respect to temperature. Almost all TC measurement setups are bespoke. They vary in the way the module is heated, how the temperature is controlled, and in the light sources used.

Both natural and simulated sunlight can be used for TC measurements. Solar simulators can have a continuous or pulsed light source with a varying quality of the spectrum. The IEC 60891 standard allows for class BBB solar simulators to be used for TC measurements. To enable the comparison of TCs at different irradiance levels and under different spectra, the TCs are normalized by the value of the respective parameter (either from the measurement or better from the linear fit to the data) at 25 °C and reported in %/°C.

The large deviation in the measurements is mostly due to the temperature control of the module and the uncertainty in the temperature measurement. There is a large variability in how modules are heated, how the temperature homogeneity is ensured, and in when and where the temperature is measured.

The heat transfer to the module can be via convection, conduction, radiation, or a combination of the above. It can also be directional from the back or front of the module, or from all directions. The way the uniformity of the module temperature is achieved also varies, for example, via insulating different parts of the module (back or side and frame) or placing in a chamber with a glass window.

In addition, the effective temperature of the module (defined as the equivalent temperature at which the module would have the same performance parameters as if it were perfectly uniform in temperature) is estimated in completely different ways. Most commonly, the temperature is measured at the back of the module; however, the location of the measurements and the number of points measured and averaged varies widely. IEC 60891, which defines the determination of TCs, requires four temperature sensors, whereas IEC 61853-1 [14] requires only three.

Finally, measurements can be taken both as modules heat up and as they cool down, either while the module temperature is continuously changing (on-the-fly measurement), or the module can be stabilized at various temperatures before a measurement is taken (stepwise measurement).

In the case of continuous light sources being used, including natural sunlight, the module is shaded until it reaches ambient temperature. Alternatively, it can be actively cooled to temperatures below ambient. The module is then unshaded and is measured as it heats up due to the incident light. For pulsed solar simulator setups, the module is in a chamber with a glass front where the temperature is controlled via convection and the module is measured as it heats up or as it cools down. Alternatively, the module can be preheated via a contact heating mat or in a chamber/oven and measured as it cools down.

The permutation of the above approaches results in many different bespoke systems that can have completely different temperature measurement uncertainty. Setups employing all the typical approaches are investigated in this paper.

III. TEMPERATURE COEFFICIENT UNCERTAINTY PROPAGATION

As with any other photovoltaic (PV) measurement, TCs have to be accompanied with an associated uncertainty calculated according to the Guide to the expression of Uncertainty in Measurement (GUM) [15] to be meaningful. In this section, the details of this calculation are presented.

TC measurements of PV modules have nonnegligible uncertainties in both the measured electrical parameter (either P_{MAX}, I_{SC}, or V_{OC}) and the effective temperature T_{EFF}. In addition, P_{MAX}, I_{SC}, and V_{OC} measurements at different temperatures are heavily correlated. One commonly adopted approach is that the systematic effects that introduce correlations are not included in the uncertainty for TC measurements. This assumes that correlations would only change the intercept of the linear fit between T_{EFF} and P_{MAX}, I_{SC} or V_{OC} but not the slope (which is the actual TC). This assumption is not true when the systematic effects are proportional to the measurement rather than an offset. Almost all uncertainty sources in P_{MAX}, I_{SC}, and V_{OC} are estimated in relative terms as scaling factors, i.e., are proportional.

For the above reasons, the most general case for linear fitting and uncertainty estimation has to be used. This can be done with a generalized Gauss–Markov regression, where all measurement data have nonnegligible uncertainties and associated correlations. More details about the different types of regression and the underlying assumptions for which they are appropriate can be found in [16]. In Clause 10 of ISO/TS 28037:2010 [17], an algorithm for a generalized Gauss–Markov regression and calculating the uncertainty of the fit is presented. An implementation of this algorithm by the National Physical Laboratory (NPL) [18] is used by the authors to calculate the uncertainty of PV TC measurements. The algorithm requires vectors of measurements $\vec{P}$ and $\vec{T}$ and variance–covariance matrices U_P and U_T as inputs. It yields the intercept a, the slope b (i.e., the TC), their variances (squared uncertainties) $u^2(a)$ and $u^2(b)$, and the covariance between the two $\mathrm{cov}(a,\ b)$. The derivation of the uncertainty equations used in the technical specification are available in [16, App. D]. The aim of this paper is to bring measurements into agreement within the calculated uncertainty by incorporating the variance–covariance matrices into the calculation of the uncertainty of relative TCs.

In order to provide sufficient detail of the uncertainty calculation methodology of P_{MAX} TC–δ, the uncertainties of the TCs for I_{SC} and V_{OC} are not addressed explicitly in this work, as this would lengthen the paper significantly. However, there is sufficient information for these to be inferred. The uncertainty sources for P_{MAX} measurements are a combination of the uncertainty sources for I_{SC} and V_{OC} measurements. The temperature measurement uncertainty and the propagation methodology are identical for all three TCs.

A. Temperature Uncertainty

The TC of maximum power can be defined as the slope b in

$$P_{\mathrm{MAX}} = a + T_{\mathrm{EFF}} * b \qquad (1)$$

where T_{EFF} is the temperature of the module if it were perfectly uniform. The measurement model for T_{EFF} is

$$T_{\mathrm{EFF}} = T_b + e_{\mathrm{CAL}} + e_{\mathrm{DAQ}} + e_{\mathrm{BtoJ}} + e_{\mathrm{hom}} \tag{2}$$

where T_b is the indicated module temperature at the middle back. This could also be the average of a number of temperature measurements at the back of the module. The other input quantities e_* are effects that introduce significant uncertainty components in T_{EFF}, i.e., sources of uncertainty due to the following:

e_{CAL} uncertainty in temperature sensor (PT100) calibration;
e_{DAQ} imperfect data acquisition (DAQ);
e_{BtoJ} difference in temperature between the junction and back of module;
e_{hom} temperature nonhomogeneity of the module.

In the model above, i.e., (2), the T_{EFF} and the uncertainty sources are all in °C.

Each of these input quantities is described by a probability density function (pdf). Repeatability measurements could be used for Type A estimate, according to the GUM, to assign a pdf for T_b due to random effects. In this work, e_{DAQ} includes these random effects. This is only the case if it has been estimated in that way and care must be taken not to miss or to double count this effect. All T_{EFF} uncertainty sources are estimated via Type B methods. Noting that the sensitivity coefficients are all equal to 1, the standard uncertainty of each temperature measurement can be calculated as

$$u_{T\,\mathrm{EFF}} = \sqrt{u_{\mathrm{CAL}}^2 + u_{\mathrm{DAQ}}^2 + u_{\mathrm{BtoJ}}^2 + u_{\mathrm{hom}}^2} \tag{3}$$

where u_* is the standard deviation (also standard uncertainty) corresponding to each of the uncertainty sources e_* listed above.

In (3), no correlation is assumed between individual uncertainty sources at a given nominal temperature. For example, the temperature nonuniformity of the module at 50 °C does not affect the difference in temperature between the back of the module and the PV junction at the location where the temperature is measured. This assumption would not always be true. The way the module is heated would affect this, for example, if the module is heated very quickly from the front, it is possible that both the temperature nonuniformity and back-to-junction difference would be larger than if the module is heated slowly. If nonnegligible correlations are expected, (3) needs to be modified to include them. Estimating the uncertainty contributors repeatedly can be used to estimate the correlation between the two effects.

To calculate the uncertainty in T_{EFF} according to the GUM, all input quantities have to be symmetrical, i.e., all corrections applied. All effects e_* should have an expectation value (mean) of 0 and standard deviation (also standard uncertainty) u_*. Depending on the measurement setup, e_{BtoJ} and e_{hom} are likely not to be centered on 0, i.e., a correction is required. Corrections can be treated as input quantities [19]. Assuming they are centered on $C_{e\mathrm{BtoJ}}$ and $C_{e\mathrm{hom}}$, these can be described as

$$e_{\mathrm{BtoJ}}^* = e_{\mathrm{BtoJ}} - C_{e\mathrm{BtoJ}} \tag{4}$$

and

$$e_{\mathrm{hom}}^* = e_{\mathrm{hom}} - C_{e\mathrm{hom}}. \tag{5}$$

e_{BtoJ}^* and e_{hom}^* can be described by normal distributions centered on 0 and with standard deviations $u_{\mathrm{BtoJ}*}$ and $u_{\mathrm{hom}*}$, respectively. Note $u_{\mathrm{BtoJ}*}$ and $u_{\mathrm{hom}*}$ include the uncertainty of the corrections. Equation (2) becomes

$$T_{\mathrm{EFFc}} = T_b + C_{\mathrm{BtoJ}} + C_{e\mathrm{hom}} + e_{\mathrm{CAL}} + e_{\mathrm{DAQ}} + e_{\mathrm{BtoJ}}^* + e_{\mathrm{hom}}^*. \tag{6}$$

Equation (6) is the model for effective temperature when a correction is applied, i.e., T_{EFFc}. The uncertainty of the corrected effective temperature $u_{T\,\mathrm{EFFc}}$ is

$$u_{T\,\mathrm{EFFc}} = \sqrt{u_{\mathrm{CAL}}^2 + u_{\mathrm{DAQ}}^2 + u_{\mathrm{BtoJ}*}^2 + u_{\mathrm{hom}*}^2}. \tag{7}$$

While not recommended, it is often the case that a correction due to a systematic effect is not applied, since the uncertainty of the correction is relatively large compared with the correction itself. It is somewhat less critical to "expand" the uncertainty compared with applying a correction to the measurement results. How to "expand" this uncertainty is a subject of debate. The methods for "expanding" the uncertainty when a correction is not applied are reviewed in [20]. If $|C_*| < u_{T\,\mathrm{EFFc}}$, then the RSSu approach presented in [21] can be used for its simplicity and symmetry. In that case, (3) becomes

$$\begin{aligned} &u_{T\,\mathrm{EFF}} \\ &= \sqrt{u_{\mathrm{CAL}}^2 + u_{\mathrm{DAQ}}^2 + C_{\mathrm{BtoJ}}^2 + C_{e\mathrm{hom}}^2 + u_{\mathrm{BtoJ}*}^2 + u_{\mathrm{hom}*}^2}. \end{aligned} \tag{8}$$

The uncertainty components can be divided into those due to systematic effects u_S and those due to random effects u_R in the context of consecutive measurements at different temperatures

$$u_{T_{\mathrm{EFF}}}^2 = u_S^2 + u_R^2. \tag{9}$$

In accordance with Appendix D of ISO/TS 28037:2010, the covariance between any two measurements at different nominal temperatures is

$$\mathrm{cov}\left(T_{\mathrm{EFF}_i},\ T_{\mathrm{EFF}_j}\right) = u_{\mathrm{Sij}}^2 \tag{10}$$

and the variance–covariance matrix $\boldsymbol{U}_{T_{\mathrm{EFF}}}$ is

$$\boldsymbol{U}_{T_{\mathrm{EFF}}} = \begin{bmatrix} u_S^2 + u_{R1}^2 & u_{\mathrm{Sij}}^2 & \cdots & u_{\mathrm{Sij}}^2 \\ u_{\mathrm{Sij}}^2 & u_S^2 + u_{R2}^2 & \cdots & u_{\mathrm{Sij}}^2 \\ \vdots & \vdots & \ddots & \vdots \\ u_{\mathrm{Sij}}^2 & u_{\mathrm{Sij}}^2 & \cdots & u_S^2 + u_{Rn}^2 \end{bmatrix}. \tag{11}$$

Estimating the correlation between the measurements and thus the covariance requires in-depth analysis of the specific measurement system. In practice, most uncertainty sources might have both a systematic and a random component. In addition, not applying a correction and "expanding" the uncertainty instead complicates the covariance estimates further. The following estimates hold true for the systems considered in this work, for which corrections were not applied:

$$\begin{aligned} u_{\mathrm{Sij}}^2 = {}& u_{\mathrm{CAL}}^2 + \mathrm{cov}\left(C_{\mathrm{BtoJi}}, C_{\mathrm{BtoJj}}\right) \\ &+ \mathrm{cov}\left(C_{\mathrm{ehomi}}, C_{\mathrm{ehomj}}\right) \end{aligned} \tag{12}$$

and

$$u_{\text{Ri}}^2 = u_{\text{DAQ}}^2 + u_{\text{BtoJ}*}^2 + u_{\text{hom}*}^2 + C_{\text{BtoJ}}^2 + C_{\text{ehom}}^2 \\ - \text{cov}\left(C_{\text{BtoJi}}, C_{\text{BtoJj}}\right) \\ - \text{cov}\left(C_{\text{ehomi}}, C_{\text{ehomj}}\right) \tag{13}$$

where

$$\text{cov}\left(C_{*i}, C_{*j}\right) \cong \text{sign}\left(C_{*i}\right) \times \text{sign}\left(C_{*i}\right) \\ \times \min\left(|C_{*i}|, |C_{*j}|\right)^2. \tag{14}$$

The systems in this work for which a correction was not applied all had positive $\text{cov}(C_{*i}, C_{*j})$, i.e., the systematic effects were estimated in the same direction for all temperatures. From (12) and (13), neglecting these covariances results in smaller estimates for $u_{\text{Si},j}^2$ and larger estimates for u_{Ri}^2, which, in turn, results in a larger overall uncertainty $u(b)$. Therefore, for the systems considered, it is possible to neglect $\text{cov}(C_{*i}, C_{*j})$, resulting in a conservative uncertainty estimate.

B. Details of Estimating e_{BtoJ} and e_{hom}

In this section, the details of e_{BtoJ} and e_{hom} estimation are described. It can be assumed that

$$e_{\text{hom}}, \cong T_{\text{avr}} - T_{\text{mid}} \tag{15}$$

where T_{avr} is the average temperature at the front of the module, and T_{mid} is the temperature at the front middle of the module.

Infrared cameras can be used to estimate the temperature uniformity of modules. In this work, infrared cameras were used for Systems C and E (see Section IV). For these systems, the modules were measured in a large air-conditioned room mounted vertically resulting in a temperature gradient and thus were expected to have the largest temperature nonuniformity.

While the absolute temperature measurements of infrared cameras can have large uncertainties, i.e., as large as 20% [22], [23], they can be used in combination with PT100 measurements to estimate the pdf of this uncertainty source. After validating the infrared images with PT100 measurements, the images can be used to estimate a conservative rectangular distribution for T_{avr} and T_{mid}. In other words, a range r can be estimated so that T_{avr} and T_{mid} are samples of the interval $[T - r, T + r]$, where T is the nominal temperature defined as the average of T_{min} and T_{max} at any given measurement temperature. Note that r may be different for T_{avr} and T_{mid}. It must also be noted that infrared images have definitional uncertainty related to where the border for calculating $T_{\text{min}}, T_{\text{max}}$, and T_{avr} is defined. Since T_{min} is significantly affected by this, the interval ranges can be estimated relative to T_{max} instead of T. T_{max} is immune to small changes in the border definition. The interval for T_{avr} and T_{mid} should be the same, regardless of the reference point used; thus, the estimate for e_{hom} is the same.

The assigned intervals approximated via normal distributions according to the GUM, for the case in which r is the same for T_{avr} and T_{mid}, are as follows:

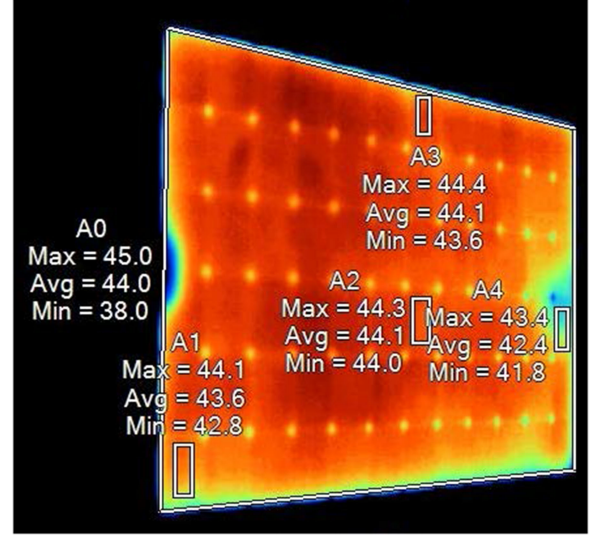$$T_{\text{avr}} = N\left(T, \frac{r}{\sqrt{3}}\right) \tag{16}$$

Fig. 1. Module temperature homogeneity according to infrared cameras. All measurements are in °C. The rectangles for which the temperature is displayed correspond to the position of monitoring the PT100s at the back, while the module is heated.

and

$$T_{\text{mid}} = N\left(T, \frac{r}{\sqrt{3}}\right). \tag{17}$$

The pdf for e_{hom} is thus

$$e_{\text{hom}} = N\left(0, \frac{r\sqrt{2}}{\sqrt{3}}\right). \tag{18}$$

In most measurement systems, characteristic patterns occur at higher temperatures, as it can be seen in Fig. 1. The middle of the module tends to be warmer than the edges. In this particular case, the cold spot on the left is due to the junction box and the one the right is due to the proximity to the Peltier element that controls the reference cell (RC) temperature. Both T_{avr} and T_{mid} are samples from the asymmetric half-interval $[T, T + r]$. If sufficient repeat measurements are taken, this interval range can be further reduced. These assumptions are setup specific. They are based on a single measurement at the middle of the module. The pdfs of uncertainty sources can be different for other systems where a number of PT100 measurements at different locations are averaged together; however, they can be treated similarly.

For the single measurement case with asymmetrical interval

$$T_{\text{avr}} = N\left(T + \frac{r}{2}, \frac{r}{2\sqrt{3}}\right) \tag{19}$$

and

$$T_{\text{mid}} = N\left(T + \frac{r}{2}, \frac{r}{2\sqrt{3}}\right). \tag{20}$$

Thus

$$e_{\text{hom}} = N\left(0, \frac{r\sqrt{2}}{2\sqrt{3}}\right) = N\left(0, \frac{r}{\sqrt{6}}\right) \tag{21}$$

	System C @ 25 °C	System C @ 40 °C	System C @ 60 °C
u_{CAL}	0.06 °C	0.06 °C	0.06 °C
u_{DAQ}	0.29 °C	0.29 °C	0.29 °C
C_{BtoJ}	0.29 °C	0.50 °C	0.83 °C
C_{ehom}	0.00 °C	0.00 °C	0.00 °C
$u_{\mathrm{BtoJ}*}$	0.08 °C	0.15 °C	0.83 °C
$u_{\mathrm{hom}*}$	0.36 °C	0.66 °C	1.34 °C
$u_{T\,\mathrm{EFF}}$	0.56 °C	0.89 °C	1.81 °C
u_R	0.47 °C	0.84 °C	1.78 °C
u_S	0.30 °C	0.30 °C	0.30 °C

assuming the two are not correlated. Since e_{hom} is the difference between the two, positive correlations would cancel out and, thus, reduce the uncertainty. Therefore, assuming no correlation is a conservative estimate. If negative correlations are suspected, they should be included.

The treatment for e_{BtoJ} is similar. One can assume a range based on simultaneous PT100 measurements at the back and front of the module. These measurements are done in a separate thermal cycle used for uncertainty estimation and are assumed valid for modules with a similar mechanical structure. There are no PT100 sensors in front of the module during the TC measurement. The estimated range r_2 is system dependent and can be either symmetric or asymmetric. For example, for one of the systems, the front of the module was measured to be always warmer than the back due to the radiative heating from the front. In this case T_{jun} is within $[T_b, \ T_b + r_2 \,]$, and thus

$$e_{\mathrm{BtoJ}} = N\left(\frac{r_2}{2}, \frac{r_2}{2\sqrt{3}}\right). \qquad (22)$$

The estimates for the uncertainty contribution of each of the described sources for System C with a coverage factor $k = 1$ [15] at three different temperatures are reported in Table I as an example. u_R and u_S are calculated according to (12) and (13), where $\mathrm{cov}(C_{\mathrm{BtoJi}}, C_{\mathrm{BtoJj}})$ is equal to C_{BtoJ} at 25 °C and where $\mathrm{cov}(C_{\mathrm{ehomi}}, \ C_{\mathrm{ehomj}})$ is equal to 0.

At CREST, T_{EFF} is measured separately and used for TC calculation. Before the TC measurement, the module is placed in a thermal chamber and stabilized at different temperatures. The temperature is measured with PT100s across the back and front of the module. The maximum difference in temperature is less than 0.2 °C. When the module temperature has settled, a set current (80% of the rated I_{SC}) is injected into the module and the voltage measured alongside the PT100 average temperature. This average temperature is the best estimate for T_{EFF}. These measurements are used to create a calibration curve that maps the measured voltage at the fixed injected current to the T_{EFF} of the module. For the measured modules, the underlying model was linear, and therefore, a weighted total least-squares linear fit was used. The same current is injected and the voltage recorded just before and just after flashing the module and measuring the I–V curve. The voltage measurements were then translated into an estimate for the T_{EFF} using the inverse function of the fit. The calculated T_{EFF} is used for the TC calculation and the uncertainty of the calculated T_{EFF} (the uncertainty is module

specific but approximately 0.6 °C) is propagating into the TC uncertainty. The uncertainty of the calibration curve itself is calculated from the uncertainties in the measured voltage and temperature and that of setting the injection current.

C. P_{MAX} Uncertainty

The contributions of all uncertainty sources in P_{MAX} measurements are estimated in relative terms. This is because the sensitivity coefficients are then equal to 1. This simplifies the uncertainty propagation. Details of estimating I_{SC}, V_{OC}, and P_{MAX} uncertainties at STC are published in [6]–[10]. Examples of the models that apply to most systems are

$$I_{\mathrm{RC}} = I_{\mathrm{RC0}} * e_{\mathrm{RCdaq}} * e_{\mathrm{Temp}} \qquad (23)$$

$$E_{\mathrm{rel}} = \frac{I_{\mathrm{RC}}}{RC_{\mathrm{cal}}} * e_{\mathrm{RCcal}} * e_{\mathrm{RCdrift}} * e_h * e_o * e_a \qquad (24)$$

$$I_{\mathrm{DUT}} = \frac{I_0}{E_{\mathrm{rel}}} * e_{\mathrm{Idaq}} * e_{\mathrm{MMF}} * e_{\mathrm{IFIT}} \qquad (25)$$

$$e_{V\,E} = 1 + 0.053 * ln\left(E_{\mathrm{rel}}\right) \qquad (26)$$

$$V_{\mathrm{DUT}} = V_0 * e_{V\,\mathrm{daq}} * e_{V\,E} * e_{V_{\mathrm{FIT}}} \qquad (27)$$

$$P_{\mathrm{MAX}} = I_{\mathrm{mpp}} * V_{\mathrm{mpp}} * e_{\mathrm{MPPfit}} * e_{\mathrm{FF}} \qquad (28)$$

where

I_{RC}	short-circuit current of the RC;
I_{RC0}	indicated short-circuit current of the RC;
E_{rel}	ratio of measured irradiance to 1000 W/m²;
RC_{cal}	calibrated value of RC short-circuit current at STC;
I_{DUT}	current of the device under test (DUT);
I_0	indicated current of the DUT;
V_{DUT}	voltage of the DUT;
V_0	indicated voltage of the DUT;
I_{mpp}	current of the DUT at maximum power point (MPP);
V_{mpp}	voltage of the DUT at MPP;
P_{MAX}	maximum power of the DUT;

and the uncertainty sources are due to

e_{RCdaq}	imperfect DAQ of the RC;
e_{Temp}	difference in temp of the RC from STC;
e_{RCcal}	uncertainty in the calibration of the RC;
e_{RCdrift}	drift of the calibration value since the calibration;
e_h	nonhomogeneity of irradiance;
e_o	difference in orientation of the DUT and the RC;
e_a	difference in alignment between the DUT and RC;
e_{Idaq}	imperfect current DAQ of the DUT;
e_{MMF}	mismatch factor (MMF);
e_{IFIT}	fitting uncertainty of short-circuit current;
e_{VE}	irradiance deviation affecting the voltage;
$e_{V\mathrm{daq}}$	imperfect voltage DAQ of the DUT;
$e_{V_{\mathrm{FIT}}}$	fitting uncertainty of open-circuit voltage;
e_{MPPfit}	fitting uncertainty of MPP fit;
e_{FF}	DUT contacting affecting the fill factor.

All currents are in Amperes, voltages are in Volts, and power is in Watts. Most of the above uncertainties are estimated via Type B methods or a combination of Type A and Type B methods, e.g., e_{FF}.

When estimating measurement uncertainties at STC, the uncertainties in the temperature of the DUT and the RC are translated into uncertainties in voltage and current measurements via typical TCs. In this work, both P_{MAX} and temperature uncertainties are propagated into the overall TC uncertainty. The two are treated separately. Therefore, temperature effects are not considered in P_{MAX} uncertainty. An exception is the uncertainty due to the deviation in temperature of the RC from 25 °C and is included as u_{temp}. All the uncertainty sources are assumed to be normally distributed and estimated to have an expectation value of one and an associated relative standard deviation u_*. Therefore, the expressions for the relative standard uncertainties in I_{SC}, V_{OC}, and P_{MAX} are as follows:

$$u_{I_{\mathrm{RC}}} = \sqrt{u_{\mathrm{Idaq}}^2 + u_{\mathrm{temp}}^2} \tag{29}$$

$$u_E = \sqrt{u_{I_{\mathrm{RC}}}^2 + u_{\mathrm{RCcal}}^2 + u_{\mathrm{RCdrift}}^2 + u_a^2 + u_o^2 + u_h^2} \tag{30}$$

$$u_{\mathrm{ISC}} = \sqrt{u_{I_{\mathrm{DAQ}}}^2 + u_E^2 + u_{\mathrm{MMF}}^2 + u_{I_{\mathrm{FIT}}}^2} \tag{31}$$

$$u_{VOC} = \sqrt{u_{V_{\mathrm{DAQ}}}^2 + u_{V_E}^2 + u_{V_{\mathrm{MMF}}}^2 + u_{V_{\mathrm{FIT}}}^2} \tag{32}$$

$$u_{P\mathrm{MAX}} = \sqrt{u_{V_{\mathrm{mpp}}}^2 + u_{I_{\mathrm{mpp}}}^2 + u_{\mathrm{FF}}^2 + u_{P_{\mathrm{FIT}}}^2}. \tag{33}$$

Note that $u_{V_{\mathrm{mpp}}}$ is equal to u_{VOC} and that $u_{I_{\mathrm{mpp}}}$ is equal to u_{ISC}, but without the uncertainty associated with fitting V_{OC} and I_{SC}.

Sometimes, repeatability is included as an uncertainty source to account for some of the random effects that are difficult to be estimated as separate sources with a bottom-up approach. Care must be taken not to double count. In [6], fill factor uncertainty is a Type A estimate of the effects of software, connections, and cabling that are assumed random. It is possible to include a similar source for I_{SC} and V_{OC}, if required. The uncertainty sources may not be limited to the ones listed above for different systems. For example, reflections could be nonnegligible for some setups.

Similar to temperature measurements, the sources of uncertainty can be separated into random and systematic between the sequential measurements at different temperatures

$$u_{P\mathrm{MAX}}^2 = u_{\mathrm{Sr}}^2 + u_{\mathrm{Rr}}^2 \tag{34}$$

where u_{Sr} is the relative standard uncertainty due to systematic effects and u_{Rr} is the relative standard uncertainty due to random effects. This separation is made considering consecutive measurements at different temperatures without disconnecting or moving the module.

The uncertainty in relative irradiance, u_E, is almost entirely systematic with the exception of the RC short-circuit current DAQ and temperature components combined into $u_{I_{\mathrm{RC}}}$ and assumed random. Note that the DAQ uncertainty can have a nonrandom effect related to the calibration of the DAQ itself. Due to the logarithmic relation between irradiance and voltage, the effects of the above components on voltage measurements are negligible. Therefore, the uncertainty in voltage due to irradiance is assumed fully systematic.

MMF correction is not normally applied to TC measurements. The uncertainty due to the mismatch could be assumed systematic for all measurements. This means that the change in spectral responsivity of the device with temperature [24] in combination with the spectral irradiance of the light source is assumed negligible. This may not be the case for some systems with light sources that have class B spectra. In that case, an additional component must be added to $u_{P\mathrm{MAX}}^2$ due to the change in MMF. This component has been included for all systems in this work, even though the majority had a class A spectrum. This is particularly important for I_{SC} TC measurement, as discussed in [24], where a temperature-dependent MMF correction is proposed instead of measuring the TC. The effect on voltage due to the MMF is assumed fully systematic.

The uncertainty due to connecting the module is systematic, since the module is not disconnected between measurements. In fact, this component has both a repeatability component and a connection component. It is difficult to separate between the two. A factor can be assumed and used, where a part is due to the random effects and the rest is due to contacting. Equal amounts were attributed here to repeatability and connectivity effects. As a result of the above considerations, the following equations apply:

$$u_{\mathrm{Sr}}^2 = u_E^2 - u_{I_{\mathrm{RC}}}^2 + u_{\mathrm{MMFs}}^2 + u_{V_E}^2 + u_{V_{\mathrm{MMF}}}^2 + \frac{u_{\mathrm{FF}}^2}{2} \tag{35}$$

$$u_{\mathrm{Rr}}^2 = u_{I_{\mathrm{RC}}}^2 + u_{I_{\mathrm{DAQ}}}^2 + u_{\mathrm{MMFr}}^2 + u_{V_{\mathrm{DAQ}}}^2 + u_{P_{\mathrm{FIT}}}^2 + \frac{u_{\mathrm{FF}}^2}{2} \tag{36}$$

where

$$u_{\mathrm{MMF}}^2 = u_{\mathrm{MMFs}}^2 + u_{\mathrm{MMFr}}^2 \tag{37}$$

and u_{MMFr} is estimated as the relative uncertainty in the current (and thus power) due to the change in the spectral responsivity of the module with temperature in combination with the difference between the spectrum of the light source and the standard spectrum. u_{MMFs} is the relative uncertainty due to mismatch at 25 °C.

For the variance–covariance matrix, the absolute standard uncertainties are required. The relation between the two is

$$u_{P\mathrm{MAX}_{\mathrm{abs}}} = P_{\mathrm{MAX}i} * u_{P\mathrm{MAX}}. \tag{38}$$

If P_{MAX} is substituted with p for brevity, the covariance between any two measurements is

$$\mathrm{cov}(p_i, p_j) = p_i p_j u_{\mathrm{Sr}}^2. \tag{39}$$

The variance–covariance matrix $\boldsymbol{U}_P$ is

$$\boldsymbol{U}_P =$$
$$\begin{bmatrix} p_i^2 \left(u_{\mathrm{Sr}}^2 + u_{\mathrm{Rr}}^2\right) & p_i p_j u_{\mathrm{Sr}}^2 & \cdots & p_i p_j u_{\mathrm{Sr}}^2 \\ p_i p_j u_{\mathrm{Sr}}^2 & p_i^2 \left(u_{\mathrm{Sr}}^2 + u_{\mathrm{Rr}}^2\right) & \cdots & p_i p_j u_{\mathrm{Sr}}^2 \\ \vdots & \vdots & \ddots & \vdots \\ p_i p_j u_{\mathrm{Sr}}^2 & p_i p_j u_{\mathrm{Sr}}^2 & \cdots & p_i^2 \left(u_{\mathrm{Sr}}^2 + u_{\mathrm{Rr}}^2\right) \end{bmatrix}. \tag{40}$$

TABLE II
P_{MAX} Uncertaitny Contributions at $k=1$ in % and Their Systematic and Random Components for System C

Source	Total	Random	Systematic
u_{RCdaq}	0.060%	0.060%	0.000%
u_{Temp}	0.029%	0.029%	0.000%
u_{RCcal}	0.320%	0.000%	0.320%
u_{RCdrift}	0.006%	0.000%	0.006%
u_h	0.664%	0.000%	0.664%
u_o	0.149%	0.000%	0.149%
u_a	0.046%	0.000%	0.046%
u_{Idaq}	0.023%	0.023%	0.000%
u_{MMF}	0.520%	0.100%	0.510%
$u_{I\ \mathrm{FIT}}$	0.005%	0.005%	0.000%
$u_{E\ v}$	0.004%	0.000%	0.004%
$u_{V\ \mathrm{daq}}$	0.023%	0.023%	0.000%
$u_{V\mathrm{FIT}}$	0.005%	0.005%	0.000%
u_{MPPfit}	0.010%	0.010%	0.000%
u_{FF}	0.360%	0.255%	0.255%
$u_{P\ \mathrm{MAX}}$	0.986%	0.283%	0.945%

After measuring the temperature and power (vectors $\vec{T}$ and $\vec{P}$) and estimating the systematic and random uncertainties for each, $\boldsymbol{U}_P$ and $\boldsymbol{U}_T$ can be created based on (11) and (40). These are then combined into

$$\boldsymbol{U} = \begin{bmatrix} \boldsymbol{U}_T & 0 \\ 0 & \boldsymbol{U}_P \end{bmatrix}. \tag{41}$$

a, b, $u^2(a)$, $u^2(b)$, and cov(a, b) are then calculated using NPL's software implementation [18] of the algorithm published in clause 10 of TS 28037:2010.

Measurements of the TCs of modules are taken at different irradiances; thus, usually, relative TCs in %/°C are reported. This allows an easy comparison as I_{SC} and P_{MAX} scale with irradiance. The calculated value of the module power at 25 °C is used to normalize the coefficient

$$\delta_{\mathrm{rel}} = \frac{b}{p_{25}} * 100 = \frac{b}{a + 25b} * 100. \tag{42}$$

According to the GUM, the uncertainty of the relative coefficient is

$$\begin{aligned} u^2\left(\delta_{\mathrm{rel}}\right) \\ = c^2\left(a\right) u^2\left(a\right) + c^2\left(b\right) u^2\left(b\right) + 2c\left(a\right) c\left(b\right) \mathrm{cov}\left(a,\ b\right) \end{aligned} \tag{43}$$

where the sensitivity coefficients are

$$c\left(a\right) = -\frac{100b}{\left(a + 25b\right)^2} \tag{44}$$

$$c\left(b\right) = \frac{100a}{\left(a + 25b\right)^2}. \tag{45}$$

In Table II, example estimates of the contributions of uncertainty sources for System C and their random and systematic relative components calculated according to (35) and (36) are reported.

In any intercomparisons, the measurand has to be fully defined. The calculated TCs, both relative and absolute, and their uncertainties are defined based on the T_{EFF} of the module and are applicable near STC conditions. There are other factors that

may introduce additional uncertainties when TC measurements are used for energy yield or energy rating estimates. For example, TC nonlinearity was reported in [25]. While the TCs of cells are expected to be linear in the range of 10–80 °C, it is possible to have nonlinear modules due to the interconnections between cells and their nonperfect matching. Nonlinearity in thin-film modules is also possible due to the higher series resistance of those modules and temperature-affected metastability effects. However, significant errors of the effective temperature measurements of the modules at higher temperatures can also present themselves as nonlinearity. In [26], the location of the PT100s was investigated, showing that the location and number of the PT100 made a significant difference on the average temperature measurement, which is the best estimate for the T_{EFF}. In addition, due to the different kinds of dynamic heating mechanisms, indoor and outdoor measurements resulted in different TCs. All of these highlight, once again, the need for accurate uncertainty estimation and propagation in order to enable the comparison of measurements made on different bespoke systems.

IV. INTERCOMPARISON RESULTS

Two modules, one monocrystalline (72 cells of 5 in) with European Solar Test Installation (ESTI) code EY08, and one multicrystalline (60 cells of 6 in) with ESTI code EY07, both with no significant measurement artefacts, were measured on five different TC measurement systems. The systems were as follows.

1) *System A:* An indoor measurement setup using a class AAA flash solar simulator. The measurements can be done both at 800 and 1000 W/m². The module is placed vertically in a temperature-controlled chamber with a transparent glass front window. The temperature of the box is controlled by electric resistive heaters. The temperature is typically increased from ambient temperature in 5 °C steps, and at each temperature, the module is left to stabilize (within ±0.5 °C for 5 min) before the measurement is taken. The RC is outside the temperature-controlled chamber and does not have glass in front. Irradiance correction is applied based on measurements at 25 °C with the glass window open and closed. The correction cancels out when relative TCs are calculated. There is a small uncertainty in irradiance at which the absolute TCs are measured. This correction uncertainty is due to flash-to-flash variation.

2) *System B:* An identical setup for controlling the temperature as in System A, but a different flash solar simulator of class BBB is used. The measurements were performed at 700 W/m².

3) *System C:* Another indoor setup. However, the light source is a continuous large-area solar simulator class AAA. The module is heated due to the radiation of the simulator and is measured as it heats up. The RC is mounted on a plate next to the module and is temperature controlled by a Peltier element. There are curtains to shade the module from the simulator light to allow it to stabilize at ambient temperature at the beginning of the

measurement. The ambient temperature is controlled via powerful air-conditioning units. The module is in a vertical arrangement. After the module has stabilized, the curtain is opened, and measurements are taken while the module continuously heats up (on the fly).

4) *System D:* An outdoor measurement setup, where the module is heated by natural sunlight under clear sky conditions. Before starting the measurement, the module is cooled to temperatures below ambient temperature in the shade by running tap water over its frontside surface. The module is then mounted on a solar tracker (normal direct sunlight) and measured as it heats up (on the fly). The RC is mounted on a plate parallel and near to the module. It is kept at 25 °C with a Peltier cooler.

5) *System E:* An indoor setup with a class AAA pulsed solar simulator. The module is heated up to 80 °C via a contact heating mat horizontally, and measurements are taken as the module cools down in a vertical arrangement. The ambient conditions of the room and the RC temperature are controlled via air conditioning. As defined at the end of Section III-B, effective temperature measurements are taken before and after each flash via injecting a set current and reading the voltage. The voltage is converted into effective temperature based on the prior calibration of the module in an environmental chamber.

The approach presented above was applied to all five measurement setups and the TCs and their uncertainties calculated accordingly. The purpose of the round-robin was to validate the uncertainty estimation methodology.

The international standards that address interlaboratory comparisons and describe the common performance statistics that can be reported are ISO/IEC 17043 [27] and ISO 13528 [28]. In this work, the percent difference ($D_\%$) and the En numbers are reported. $D_\%$ was reported in order to be able to compare to previous round-robin results. It was calculated as follows:

$$D_\% = \frac{x - X_{\mathrm{ref}}}{X_{\mathrm{ref}}} * 100 \qquad (46)$$

where x is the measurement result of a given system, and X_{ref} is the assigned value of the measurand, i.e., the reference value, usually taken as the mean.

Having consistent uncertainty estimation for all measurement systems allowed for the calculation of the En numbers that can be used to validate the uncertainty estimation. The En number is defined as

$$En = \frac{x - X_{\mathrm{ref}}}{\sqrt{U_{\mathrm{SYS}}^2 - U_{X_{\mathrm{ref}}}^2}} \qquad (47)$$

where U_{SYS} is the expanded uncertainty of the system, i.e., at $k = 2$, and $U_{X_{\mathrm{ref}}}$ is the expanded uncertainty of the reference value, i.e., at $k = 2$.

According to ISO/IEC 17043, $|En|$ values ≤ 1 are considered "satisfactory," and $|En|$ values > 1 are considered "unsatisfactory" indicating a further investigation is required.

For the calculation of both En and $D_\%$, the reference value X_{ref} for each module, and its uncertainty U_X, were required. The reference value chosen for this work was the weighted
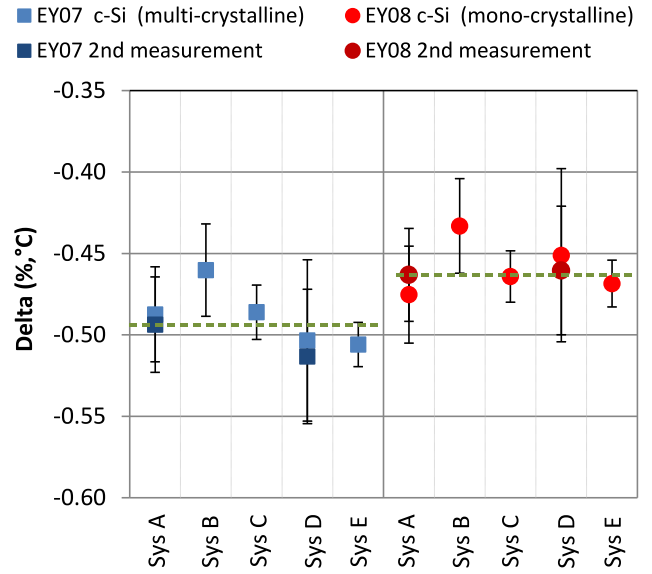

Fig. 2. TC of $P_{\max}$–Delta (δ) measurement in %/°C, their uncertainties at $k = 2$, and the weighted average as the reference value (the green-dashed line) of two different types of modules measured on five different systems each.

average (weighted by the reciprocal of the variance) as recommended in [29]. X_{ref} was calculated as follows:

$$X_{\mathrm{ref}} = \frac{\sum_i^n w_i x_i}{\sum_i^n w_i} \qquad (48)$$

where the weights were calculated as

$$w_i = \frac{1}{u_{x_i}^2}. \qquad (49)$$

The expanded uncertainty $U_{X_{\mathrm{ref}}}$ was calculated as

$$U_{X_{\mathrm{ref}}} = 2 * \frac{1}{\sqrt{\sum_i^n \frac{1}{u_{x_i}^2}}}. \qquad (50)$$

More details about the use of En numbers, weighted average, and its uncertainty in the context of PV measurement can be found in [30].

In Fig. 2, the results for the maximum power TC, δ, in %/°C are presented alongside their stated uncertainties with a coverage factor $k = 2$ and the reference value. The En numbers and $D_\%$ for each system and both modules, alongside a summary of the results, are presented in Table III.

Both modules were measured twice on system D. The original measurements were done some years earlier and are also included in Fig. 2. These measurements in conjunction with the estimated uncertainties serve to support the hypothesis that the measurand is stable. A stable measurand is a requirement for using the weighted average as the reference value. The modules were also measured both at 800 and 1000 W/m² on System A. These results are also included in Fig. 2. The results indicate that relative TCs are comparable at these irradiances.

The $D_\%$ of all δ measurements were within –6.9% to +3.9 % relative to the reference value, which is a significant improvement on previously reported module TC intercomparisons.

TABLE III
δ, $U(\delta)$ AT $k = 2$, $D_\%$ & En NUMBERS

System	EY07				EY08			
	δ, %/°C	U(δ) % of δ	$D_\%$ %	En	δ, %/°C	U (δ) % of δ	$D_\%$ %	En
A	−0.487	5.99	−1.4	0.221	−0.475	6.26	2.6	−0.387
A2	−0.494	5.93	−0.1	0.012	−0.463	6.16	−0.03	0.004
B	−0.460	6.16	−6.9	1.143	−0.433	6.70	−6.5	0.997
C	−0.486	3.44	−1.6	0.425	−0.464	3.40	0.2	−0.048
D	−0.503	9.84	1.9	−0.185	−0.451	11.8	−2.6	0.227
D2	−0.513	8.04	3.9	−0.455	−0.460	8.57	−0.6	0.070
E	−0.506	2.69	2.4	−0.736	−0.468	3.07	1.1	−0.309
Ref value	−0.494	1.74			−0.463	1.86		

TABLE IV
δ, $U(\delta)$ AT $k = 2$, $D_\%$ & En NUMBERS EXCLUDING SYSTEM B

System	EY07		EY08	
	$D_\%$, %	En	$D_\%$, %	En
A	−2.0	0.332	1.9	−0.291
A2	−0.8	0.124	−0.7	0.102
C	−2.3	0.601	−0.4	0.114
D	1.19	−0.117	−3.2	0.281
D2	3.2	−0.373	−1.2	0.143
E	1.7	−0.516	0.5	−0.133
	Ref value	$U(\delta)$	Ref value	$U(\delta)$
	−0.498	1.81	−0.466	1.94

V. DISCUSSION

One of the En values of System B is above 1, and the other is 0.997. Given the number of measurements (14 En numbers in Table III), this is slightly higher than expected, remembering that 95% of En numbers are expected to be below 1. According to the En values, all other measurements and system uncertainties were in agreement without any significant underestimation of the uncertainties.

The elevated En numbers prompted a further investigation. They are believed to be due the observed strong emission peaks of the light source used in System B. These peaks were in the spectral region where the spectral responsivity of the modules changes with temperature, i.e., where the cutoff wavelength changes in the near-infrared. The uncertainty due to the change of the MMF at different temperatures was estimated as 0.5% at $k = 1$. For the monocrystalline module EY07, the MMF at 25 °C was almost 5%. The difference in the MMF at 55 °C was calculated as an additional 1.4%. This represents an extreme case from a normal distribution with a standard deviation (uncertainty) of 0.5%, thus explaining the larger than 1 En value for that particular system. It can also be seen in Fig. 2 that system B underestimates the absolute value of the TC, which is consistent with the above.

The analysis has shown that TCs measured on system B are not fully consistent with the other systems. This is attributed to the poor spectral irradiance (class B) of this simulator. Given current state-of-the-art solar simulator technology, which makes class AAA simulators widely available, a class BBB simulator should no longer be acceptable for TC measurements. The standard IEC 60891 allows this, but a thorough analysis of the influence of a lower quality simulator on the measured TC has not been done in the past. Previous uncertainty estimations were, in many cases, overly conservative (at least double the uncertainties reported here), hiding the systematic effects of the simulator spectrum. The results reported here indicate that this influence is significant.

The detailed uncertainty analysis not only resulted in measurements that are consistent with the associated uncertainty estimates but improved the overall measurement deviation as well. If the measurement results of system B are not included, and the reference value is recalculated (see Table IV), the agreement between all measurements was ±3.2% (−2.3% to +3.2% for EY07 and −3.2% to +1.9% for EY08). This represents an improvement of up to a factor of 5 compared with previous in-

tercomparisons. This significant improvement in agreement is attributed to the consistency in which the coefficients are calculated and the use of an appropriate fitting technique given the type of measurements (weighted by both temperature and P_{MAX} uncertainty).

A comparison of the measurement deviations with the relative uncertainties, reported in Table III, indicates that the uncertainty estimate for System D could be too conservative. The uncertainty calculated and reported as part of this work already represents a reduction by a factor of 2 compared with previous estimates. System D is the outdoor measurement setup. It is expected that one or more of the input uncertainties are overestimated, and further investigations are ongoing. The most likely explanation is that the temperature nonuniformity estimate for this system was too conservative. In order to reduce this component, a more detailed investigation is required. Infrared cameras were not used outdoors and could be a way of better quantifying the temperature nonuniformity.

The temperature measurement uncertainty was a larger contributor than the uncertainties in P_{MAX}, I_{SC}, and V_{OC} for all systems. While it might be difficult to change the setup to improve the temperature control and, thus, the temperature homogeneity of the DUT, the measurement procedures can be optimized to reduce the uncertainties. This is only possible if a thorough investigation of the temperature uncertainty at different temperatures is conducted.

The uncertainty of the TC is sensitive not only to the input uncertainties but to the number of measurement points and their spread as well. System A, for example, uses a stepwise approach where the temperature is allowed to stabilize in a chamber before the measurement is taken. This generally results in better temperature homogeneity. The time required to heat up and stabilize the temperature before taking a measurement limits the number of potential measurement points. The modules were measured at four temperatures from 25 °C to 60 °C on System A, despite the recommended practice of using 5° intervals. Increasing the number of measurement points and the temperature range would reduce the uncertainty to be comparable with systems C and E but would increase the measurement time.

Systems C and E have high-temperature nonuniformity uncertainties at higher temperatures. Since the measurements are weighted by their uncertainties, there is little benefit of measuring above 70 °C. The higher temperature nonuniformity for system E is the reason for implementing the separate T_{EFF}

measurement procedure. This reduces the uncertainty significantly, but the extra step doubles the measurement time required.

VI. CONCLUSION

Previously, the reported deviation in TC measurements between laboratories was comparable or even larger than the difference in TC between modules of the same technology. In addition, TC measurement uncertainty estimation varies significantly. This is because there is no widely accepted publication that addresses the uncertainty estimation of PV TC measurements as it is the case for P_{MAX}, I_{SC}, and V_{OC} measurements. The approach used at CREST and at ESTI, which is consistent with international standards, has been presented in detail to facilitate the standardization of TC uncertainty estimation. The uncertainty analysis can be quite complex. While there are other approaches which are simpler, they can significantly over- or underestimate the uncertainties. This is because all measurements have nonnegligible uncertainties, and the nature of the measuring process results in heavily correlated measurements. This is the reason why TCs are rarely supported with uncertainty estimations and why often the measurement deviations are outside the measurement uncertainty. While the key sources of uncertainty have been discussed previously, their treatment and estimation methodology have not. The approach presented here was applied to five different bespoke measurement setups that cover most types of setups used worldwide. The measurement deviation was from –6.9% to +3.9% relative to the reference value; however, the calculated En values indicated that one of the systems had a systematic effect or an underestimated uncertainty. Further investigation confirmed that this was due to the poor spectrum of the class B simulator. Excluding the outlier measurements, the measurement deviation was reduced to ±3.2% and within stated uncertainties. This is a significant improvement compared with previously reported deviation of ±10 to ±15% and sometimes larger. The intercomparison validated the uncertainty estimation approach, while the identification of the systematic effect highlighted the importance of a robust uncertainty estimation that is not overestimated.

ACKNOWLEDGMENT

REFERENCES

[1] Y. Yang *et al.*, "Understanding the uncertainties in the measurement of temperature coefficients of Si PV modules," in *Proc. 29th Eur. Photovoltaic Sol. Energy Conf. Exhib.*, 2014, pp. 3278–3282.

[2] B. Mihaylov *et al.*, "Results of the Sophia module intercomparison part 1: STC, low irradiance conditions and temperature coefficients measurements of C-Si technologies," in *Proc. 29th Eur. Photovoltaic Sol. Energy Conf. Exhib.*, 2014, pp. 2443–2448.

[3] B. Mihaylov *et al.*, "Results of the SOPHIA module intercomparison part 2: STC, low irradiance conditions and temperature coefficients measurements of thin film technologies," in *Proc. 31st Eur. Photovoltaic Sol. Energy Conf. Exhib.*, 2015, pp. 1871–1876.

[4] K. Emery *et al.*, "Temperature dependence of photovoltaic cells, modules and systems," in *Proc. 25th IEEE Photovoltaic Spec. Conf.*, 1996, pp. 1275–1278.

[5] D. King, J. Kratochvil, and W. Boyson, "Temperature coefficients for PV modules and arrays: Measurement methods, difficulties, and results," in *Proc. 26th IEEE Photovoltaic Spec. Conf.*, 1997, pp. 1183–1186.

[6] H. Müllejans, W. Zaaiman, and R. Galleano, "Analysis and mitigation of measurement uncertainties in the traceability chain for the calibration of photovoltaic devices," *Meas. Sci. Technol.*, vol. 20, no. 7, Jul. 2009, Art. no. 075101.

[7] K. Emery, "Uncertainty analysis of certified photovoltaic measurements at the national renewable energy laboratory," Nat. Renewable Energy Lab., Golden, CO, USA, Tech. Rep. NREL/TP-520-45299, Aug. 2009.

[8] D. Dirnberger and U. Kraling, "Uncertainty in PV module measurement—Part I: Calibration of crystalline and thin-film modules," *IEEE J. Photovoltaics*, vol. 3, no. 3, pp. 1016–1026, Jul. 2013.

[9] F. Plag *et al.*, "Comprehensive analysis of a pulsed solar simulator to determine measurement uncertainty components," in *Proc. 29th Eur. Photovoltaic Sol. Energy Conf. Exhib.*, 2014, pp. 2435–2442.

[10] V. Fakhfouri *et al.*, "Uncertainty assessment of PV power measurement in industrial environments," in *Proc. 26th Eur. Photovoltaic Sol. Energy Conf. Exhib.*, 2011, pp. 3408–3412.

[11] K. Emery, "Calibration and rating of photovoltaics," in *Proc. 38th IEEE Photovoltaic Spec. Conf.*, 2012, pp. 769–774.

[12] *Photovoltaic Devices—Procedures for Temperature and Irradiance Corrections to Measured I-V Characteristics*, IEC Std. 60891, 2010.

[13] B. Mihaylov, M. Bliss, T. R. Betts, and R. Gottschalg, "Temperature coefficient measurements of PV modules and uncertainty analysis," in *Proc. Photovoltaic Sci. Appl. Technol. Conf.*, 2014, vol. 10, pp. 5–8.

[14] *Photovoltaic (PV) Module Performance Testing and Energy Rating—Irradiance and Temperature Performance Measurements and Power Rating*, IEC Std. 61853-1, 2011.

[15] *Evaluation of Measurement Data–Guide to the Expression of Uncertainty in Measurement*, ISO/IEC Guide 98-3, 2008.

[16] M. Cox, "The classification and solution of regression problems for calibration," Nat. Phys. Lab., Teddington, U.K., Rep. CMSC 24/03, 2004.

[17] *Determination and Use of Straight-Line Calibration Functions*, ISO/TS Std. 28037, 2010.

[18] I. Smith and P. Harris, *NPL's Software to Support ISO/TS 28037:2010(E)*, 2010.

[19] F. Pavese, "Corrections and input quantities in measurement models," *Int. J. Metrol. Quality Eng.*, vol. 3, no. 3, pp. 155–159, 2012.

[20] B. Magnusson and S. Ellison, "Treatment of uncorrected measurement bias in uncertainty estimation for chemical measurements," *Analytical Bioanalytical Chem.*, vol. 390, no. 1, pp. 201–213, 2008.

[21] I. H. Lira and W. Wöger, "Evaluation of the uncertainty associated with a measurement result not corrected for systematic effects," *Meas. Sci. Technol.*, vol. 9, no. 6, pp. 1010–1011, 1999.

[22] *Size-of-Source Effect in Infrared Thermometers Measuring the SSE During Calibration, MSL Tech. Guide 26*, 2012.

[23] *Focus Effect in Thermal Imagers, MSL Tech. Guide 29*, 2012.

[24] C. R. Osterwald *et al.*, "Temperature-dependent spectral mismatch corrections," *IEEE J. Photovoltaics*, vol. 5, no. 6, pp. 1692–1697, Nov. 2015.

[25] M. Schweiger, S. Michalski, U. Jahn, W. Herrmann, and U. Rau, "Nonlinearity of temperature coefficients, equivalent cell temperature and temperature behaviour of different PV-module technologies," in *Proc. 28th Eur. Photovoltaic Sol. Energy Conf. Exhib.*, 2013, pp. 3265–3268.

[26] C. W. Hansen, M. Farr, and L. Pratt, "Correcting bias in measured module temperature coefficients," in *Proc. 40th IEEE Photovoltaic Spec. Conf.*, 2014, pp. 2651–2655.

[27] *Conformity Assessment—General Requirements for Proficiency Testing*, ISO/IEC Std. 17043, 2010.

[28] *Statistical Methods For Use In Proficiency Testing By Interlaboratory Comparison*, ISO Std. 13528, 2015.

[29] M. G. Cox, "The evaluation of key comparison data," *Metrologia*, vol. 39, no. 6, pp. 589–595, Dec. 2002.

[30] H. Müllejans, W. Zaaiman, and E. D. Dunlop, "Reduction of uncertainties for photovoltaic reference cells," *Metrologia*, vol. 52, no 5, pp. 646–653, Sep. 2015.